ICIC Express Letters
Part B: Applications
Volume **7**, Number **10**, October **2016**

ICIC International ©2016 ISSN 2185-2766
pp. **2135–2142**

DOUBLE VARIABLE SPLITTINGS AND ALTERNATING OPTIMIZATION FOR IMAGE RECOVERY UNDER UNKNOWN BOUNDARY CONDITIONS

Su Xiao, Fangzhen Ge and Ke Shen

School of Computer Science and Technology
Huaibei Normal University
No. 100, Dongshan Road, Huaibei 235000, P. R. China
csxiaosu@163.com

Received March 2016; accepted June 2016

Abstract. *In real imaging systems, boundary conditions (BCs) are generally non-periodic and unknown. However, most studies adopt a periodic BC to efficiently solve image recovery problems. The fact that ring artifacts will inevitably appear in recovered images under a periodic BC cannot be disregarded. To handle this tricky problem, this paper presents a novel image recovery approach under an unknown BC. The approach focuses on addressing the image recovery problem expressed as a regularized optimization problem with a non-quadratic edge-preserving and noise-suppressing regularizer. The blur is cast as the product of a mask matrix with a circulant matrix. Thus, the operations between matrices cannot be implemented using fast Fourier transform, which requires iterative solvers. To deal with this difficult issue, double variable splitting is employed to convert the original image recovery problem into its equivalent constrained form, which is then decomposed into a series of subproblems by the alternating optimization. Alternately computing these subproblems without inner iterations obtains the closed-form solution of the original image recovery problem. In the simulation experiment, two observed benchmark images under an unknown BC with uniform blur are recovered to validate the effectiveness of the presented approach. Comparisons of the recoveries, improved signal-to-noise ratio, and speed demonstrate the superior performance of the presented approach.*

Keywords: Image recovery, Unknown BC, Observation model, Double variable splittings, Alternating optimization

1. **Introduction.** Image degradation can be represented by the linear system $y = Kx+n$, where $x \in R^N$ denotes the vector form of the latent sharp image of size $m \times n$, $y \in R^M$ represents the vector form of the observed image of size $l \times p$, $K \in R^{M\times N}$ is a linear operator, and $n \in R^M$ is an additive Gaussian noise. Given that an observed image is created by the convolution between a sharp image and a point spread function, the observed image y not only depends on the pixels in the domain of the sharp image x, but also on those outside the domain of x. Thus, the assumptions, which are usually called boundary conditions (BCs), should be made on the pixels out of the domain of sharp images. Among the various BCs, periodic BC [1] is probably the most popular for image recovery approaches. This BC supposes that the pixels in the domain of an image are orderly and circularly used to pad the domain outside the image. Thus, the corresponding linear operator K is a block-circulant-circulant-block blur matrix, which means that the fast Fourier transform (FFT)-based acceleration and non-iterative subsystem solution are feasible in image recovery. At present, most image recovery approaches, including many state-of-the-art ones [2-7], adopt periodic BC because of the simplicity and efficiency it brings to these approaches. Under periodic BC, image recovery is uniformly modeled as the regularized optimization problem: $\min_x f(x) + \mu\Phi(Px)$ (**P1**), where $f(x)$ is the data-fidelity term, constant $\mu > 0$ is the regularization parameter, $\Phi(Px)$ is the regularizer,

and $P \in R^{L \times N}$ is a sparsity-inducing operator. Iterative shrinkage or thresholding (IST) [2,3] and augmented Lagrangian (AL) [4-7], especially the latter, are popular methods to solve problem **P1**. AL method uses FFT to invert the Hessian matrices and non-iterative solvers for subproblems, and thus achieves high efficiency in recovering blurred images with low-level noise. However, for image recovery approaches under the periodic BC, completely avoiding the ring artifacts in recovered images is impossible because of the image discontinuities caused by the periodic extension of the boundaries.

The assumption on a periodic BC is generally rarely satisfied in real imaging systems. Actually, the outside pixels of latent sharp images are unknown in general cases because of the limited support domains of images; that is, the BCs are generally unknown. Under an unknown BC, FFT cannot be directly applied and iterative solvers are needed for subsystem problems because the blur operators are non-circular. Thus, under non-periodic BCs, the IST and AL methods are not suitable for image recovery problems and their performances cannot be maximized. A few approaches [8-10] have been presented to solve image recovery problems under unknown BCs. In literature [8], the image recovery problem under an unknown BC is treated as image deconvolution with inpainting and is solved by optimizing the total variation model [11] directly. In Reeves's approach [9], Tikhonov technology is adopted to regularize image recovery, and conjugate gradient (CG) iterations are used to apply FFT to matrix inversion. Recently, Sorel [10] improved the approach in [9] with non-quadratic regularization and variable splitting. Although the image recovery approaches under unknown BCs successfully avoid ring artifacts, most of these approaches are generally computationally inefficient. The reason behind this limitation is that solvers are generally needed to deal with smaller systems first to apply FFT and non-iterative inversions of matrices. Thus, the efficiencies of image recovery approaches under unknown BCs must still be improved.

Motivated by the research on image recovery under unknown BCs and based on the true characteristics of imaging systems, this paper presents a novel image recovery approach under an unknown BC to eliminate ring artifacts. Compared with existing similar approaches, the presented approach exhibits the following advantageous properties. 1) The blur is realistically modeled as the product of a mask matrix with a circulant matrix; therefore, the unknown boundary pixels can be accurately estimated together with image recovery. 2) Since the mask and the circulant matrix can be decoupled by double variable splittings, no iterative solvers are required for subproblems generated by alternately optimizing the proposed image recovery problem. 3) The closed-form solutions of the subproblems can be efficiently derived by means of non-iterative methods. Thus, the presented approach demonstrates a good performance on efficiency. 4) The presented approach has the same desirable properties as the alternating optimization-based approaches, e.g., formally confirmed convergence. The rest of this paper is arranged as follows. In Section 2, a new problem is proposed to model the image recovery according to the observation model under an unknown BC. In Section 3, a novel image recovery approach is presented based on the effective handling of the proposed problem by using double variable splittings and alternating optimization. In Section 4, comprehensive experiments are conducted to verify and evaluate the presented approach. In Section 5, the results of this paper are summarized.

2. Problem Formulation.

Under a periodic BC, $f(x)$ generally takes the following form:

$$\frac{1}{2}||y - Kx||_2^2 \tag{1}$$

with circular blur operator K. Based on the discussion above, the unknown BC, which functions well with the features of real imaging systems, should be adopted to avoid unpleasant artifacts. To model the blur operator under an unknown BC, K is supposed

to be the product of a mask matrix H with a circulant matrix B, namely, $K = HB$. Thus, the observation model can be re-expressed as

$$y = HBx + n, \tag{2}$$

where $B \in R^{Q\times N}$ represents the convolution with a blur kernel, and $H \in R^{M\times Q}$ is the truncation of an identity matrix. If the size of the support of a blur kernel is $(2a+1)(2b+1)$, as shown in Figure 1, H removes the outermost $2a$ rows and $2b$ columns of the pixels of image Bx. The mask matrix is used to exclude the blurred pixels that depend on the unknown pixels outside the domain of the latent sharp image x. Thus, M is less than N. According to Equation (2), under an unknown BC, **P1** has the following form:

$$\min_x \frac{1}{2}||y - HBx||_2^2 + \mu\Phi(Px) \tag{3}$$

which is the image recovery problem to be solved by this study.

(a) (b)

FIGURE 1. Demonstration of the sharp image and the corresponding observed image under the observation model denoted by Equation (2): (a) an image of size 256×256 (100% scale) and (b) the corresponding observed image of size 240×240 (100% scale)

For image recovery problems, regularizers must preserve the details of recovered images while suppressing the noise in the images to obtain state-of-the-art recovered results. Regularizers are currently classified into two categories: quadratic and non-quadratic. Compared with non-quadratic regularizers, quadratic regulizers prefer recovering smooth images with unsharp edges. Thus, total variation (TV) norm and frame analysis (FA) norm are best options for regularizer $\Phi(Px)$ because of their outstanding performances in image recovery [12]. Problem (3) can be expressed as

$$\min_x \frac{1}{2}||y - HBx||_2^2 + \mu||\nabla x||_1 \tag{4}$$

and

$$\min_x \frac{1}{2}||y - HBx||_2^2 + \mu||W^T x||_1, \tag{5}$$

respectively with TV norm and FA norm, where ∇ is the gradient operator, which is the same as that defined in literature [13]; W^T represents a tight frame, and if it is normalized, $W^T W = I$ is satisfied [14].

3. **Presented Approach.** The cost function of the problem cannot be minimized directly because it is non-quadratic. In addition, under unknown BCs, most methods that are used under periodic BCs cannot be directly applied to problem (3). To make the problem solvable, variable splitting [15], which is the most popular strategy at present, can be

employed. Through standard variable splitting technology, problem (3) is formulated as an equivalent constrained form:

$$\begin{aligned} &\min_{x,z} \frac{1}{2}||y - HBx||_2^2 + \mu\Phi(z) \\ &\text{s.t.} \quad z = Px, \end{aligned} \tag{6}$$

where $z \in R^L$ is a newly introduced auxiliary variable. With alternating optimization, the constrained problem (6) can be decoupled into the following subproblems:

$$x^{k+1} = \underset{x}{\operatorname{argmin}} ||y - HBx||_2^2 + \lambda||z^k - Px||_2^2, \tag{7}$$

$$z^{k+1} = \underset{z}{\operatorname{argmin}} \mu\Phi(z) + \frac{\lambda}{2}||z - Px^{k+1}||_2^2. \tag{8}$$

In this case, the optimal solution of original problem (3) can be obtained by alternately computing the two subproblems.

The cost function of problem (7) is smooth, and its direct minimization generates the following closed-form solution:

$$x^{k+1} = \left(B^T H^T HB + \lambda P^T P\right)^{-1} \left(B^T H^T y + \lambda P^T z^k\right). \tag{9}$$

$H^T H$ has no structural features that enable the direct application of FFT. Thus, preconditioned CG (PCG) can be employed as an alternative to iteratively calculate Equation (9). For subproblem (8) $\Phi(\cdot)$ is l_1-norm (i.e., $||\cdot||_1$), that is, this subproblem is an $l_1 - l_2$ denoising problem, because the TV and FA norms are adopted as regularizers in this work. Recent studies indicate that the most suitable method to address these problems is proximal mapping [16].

Through PCG, solving Equation (9) may converge to a feasible solution. The solution cannot be guaranteed to be exact, and the iterative update of x^* slows down the convergence. To avoid these disadvantages with a fast and accurate non-iterative update of x^*, this paper proposes a novel double variable splittings strategy where the problem (3) is equivalently reformulated as

$$\begin{aligned} &\min_{u,z} \frac{1}{2}||y - Hu||_2^2 + \mu\Phi(z) \\ &\text{s.t.} \quad u = Bx,\ z = Px, \end{aligned} \tag{10}$$

where $u \in R^Q$ is an auxiliary variable. Alternating optimization can decompose the constrained problem (10) into the following subproblems:

$$x^{k+1} = \underset{x}{\operatorname{argmin}} \gamma||u^k - Bx||_2^2 + \lambda||z^k - Px||_2^2, \tag{11}$$

$$u^{k+1} = \underset{u}{\operatorname{argmin}} ||y - Hu||_2^2 + \gamma||u - Bx^{k+1}||_2^2, \tag{12}$$

$$z^{k+1} = \underset{z}{\operatorname{argmin}} \mu\Phi(z) + \frac{\lambda}{2}||z - Px^{k+1}||_2^2. \tag{13}$$

Subproblems (11) to (13) clearly show that double variable splittings not only decouple the non-quadratic and quadratic parts of problem (3), but also decouple the operators H and B. The benefits of this "double decouplings" will be demonstrated when dealing with problem (3) by alternately computing the subproblems above.

The cost functions of subproblems (11) and (12) are smooth. Thus, the closed-form solutions can be directly obtained as

$$x^{k+1} = \left(\gamma B^T B + \lambda P^T P\right)^{-1} \left(\gamma B^T u^k + \lambda P^T z^k\right) \tag{14}$$

and

$$u^{k+1} = \left(\gamma I + H^T H\right)^{-1} \left(\gamma Bx^{k+1} + H^T y\right) \tag{15}$$

As stated above, subproblem (13) can be addressed by proximal mapping, where the proximity operator (i.e., close-formed solution) of this subproblem is the soft-thresholding function [17], which is:

$$soft\left(Px^{k+1}, \frac{\mu}{\lambda}\right) = \underset{z}{\operatorname{argmin}}\, \mu\Phi(z) + \frac{\lambda}{2}||z - Px^{k+1}||_2^2 \tag{16}$$

where $soft\left(\cdot, \frac{\mu}{\lambda}\right)$ represents the element-wise application of the function $s \mapsto sign(s)\max\left(|s| - \frac{\mu}{\lambda}, 0\right)$.

Based on Equations (14) to (16), the presented approach is summarized as follows:

(1) **Input**: γ, λ, and μ; H, B, and P; u^0 and z^0
(2) **Precompute**: H^TH, B^TB, P^TP, and H^Ty
(3) **For** $k = 0$ to $K_{\max}$
  a. $x^{k+1} = \left(\gamma B^TB + \lambda P^TP\right)^{-1}\left(\gamma B^Tu^k + \lambda P^Tz^k\right)$
  b. $u^{k+1} = \left(\gamma I + H^TH\right)^{-1}\left(\gamma Bx^{k+1} + H^Ty\right)$
  c. $z^{k+1} = soft(Px^{k+1}, \frac{\mu}{\lambda})$
  d. **If** the stopping criterion is satisfied
    (i) Stop iteration;
  e. **Endif**
(4) **Endfor**
(5) **Output**: x^{k+1}

The presented approach is based on double variable splittings and alternating optimization, and is thus referred to as DVSAO. In the DVSAO framework, B^TB, B^Tu^k, and Bx^{k+1} can all be calculated through FFT, and corresponding computing costs are all $O(n\log n)$. $\left(\gamma I + H^TH\right)$ is a diagonal matrix and the computing costs of $\left(\gamma I + H^TH\right)^{-1}$ and H^Ty are both $O(n)$ because H is the truncation of an identity matrix. Depending on whether P is the gradient operator or a tight frame, P^Tz^k has a computing cost of $O(n\log n)$ and P^TP has a computing cost up to $O(n\log n)$. The soft function computes z^{k+1} component-by-component; thus, its computing cost is $O(n)$. The analysis above indicates that the presented approach will achieve high running efficiency.

4. **Numerical Results.** In this section, the recoveries on the observed images illustrated in Figures 2(c) and 2(d) are performed to support the validity of the presented DVSAO approach. To produce the observed images according to Equation (2), the uniform blur of size 17×17 (i.e., $a = 8$, $b = 8$) is used. As mentioned in Section 2, the corresponding observed images are smaller compared with the sharp images illustrated in Figures 2(a) and 2(b) because the mask matrix removes a certain width of outermost pixels from the blurred images. The blurred signal-to-noise ratio (BSNR) defined as

$$BSNR = 10 \times \log_{10} \frac{||x - E\{x\}||_2^2}{N\sigma^2} \tag{17}$$

is adopted to measure the degradation degrees of the observed images, where σ^2 is the variance of the noise and $E\{x\}$ is the mean of x. To evaluate the presented approach by comparison, the approach based on variable splitting and PCG (VSPCG), which was mentioned in Section 3, is introduced as the competitor. Notably, techniques that are similar to VSPCG were also adopted in literature [9,10]. All the approaches (i.e., VSPCG and DVSAO) are run on a laptop with a Windows 7 operating system, Intel Core i5 CPU @ 2.40 GHz, 4 GB RAM, and MATLAB R2012b.

To ensure that the real performances of all approaches are well demonstrated, the parameters of these approaches are empirically configured as follows: 1) $\gamma = 1 \times 10^{-2}$, $\lambda = 2 \times 10^{-5}$, and $\mu = 8 \times 10^{-7}$ for DVSAO_TV (DVSAO approach with TV norm as the regularizer); 2) $\gamma = 1 \times 10^{-2}$, $\lambda = 2 \times 10^{-5}$, and $\mu = 5 \times 10^{-7}$ for DVSAO_FA (DVSAO

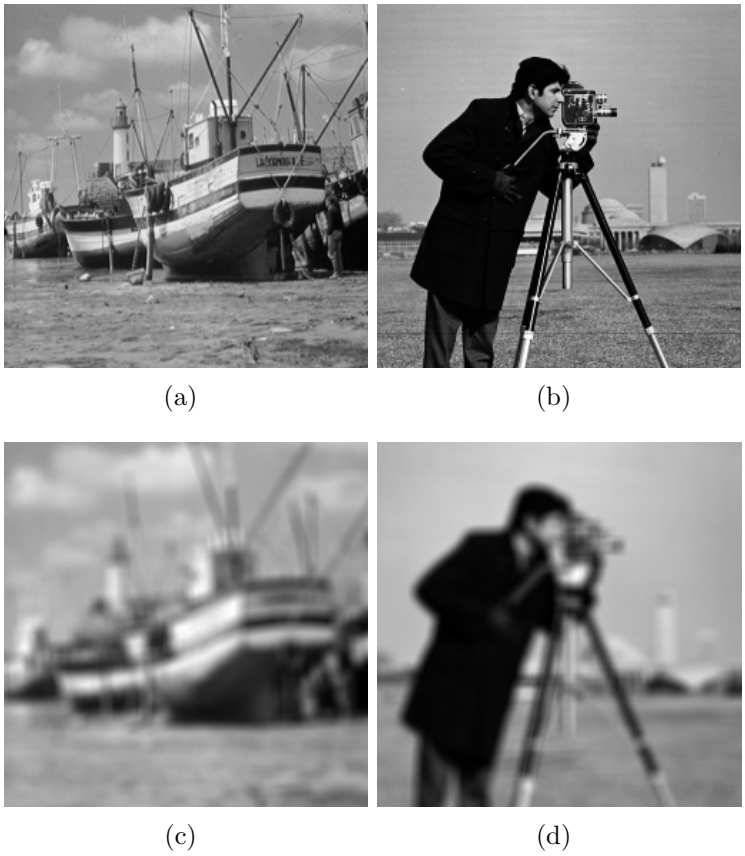

(a) (b)

(c) (d)

FIGURE 2. Sharp benchmark images and the corresponding observed images: (a) boat image of size 256×256, (b) cameraman image of size 256×256; (c) observed boat image with BSNR = 40 dB, (d) observed cameraman image with BSNR = 40 dB. All the observed images have a 240 × 240 size.

approach with FA norm as the regularizer); and 3) $\gamma = 1 \times 10^{-3}$, $\lambda = 1 \times 10^{-4}$, and $\mu = 5 \times 10^{-5}$ for both VSPCG_TV (VSPCG approach with TV norm as the regularizer) and VSPCG_FA (VSPCG approach with FA norm as the regularizer). For VSPCG_FA and DVSAO_FA, P is the redundant Haar frame, which is known to produce better recoveries. The stopping criteria of all approaches are uniformly set to "$\left(||x^{k+1} - x^k||_{fro}/||x^k||_{fro}\right) < 1 \times 10^{-4}$ or $k \geq 100$". To fairly compare the performances of all approaches, the improved signal-to-noise ratio (ISNR), which is defined as

$$ISNR = 10 \times \log_{10} \frac{||x - y||_2^2}{||x - x^{k+1}||_2^2} \tag{18}$$

is employed as the metric of the quality of recovered images. Normally, higher ISNR values indicate better recovered results.

The recovered images of all approaches are shown in Figure 3, and the corresponding ISNR values are reported in Table 1. These results evidently indicate that the presented DVSAO approach is feasible and effective, the missing edges and textures are properly reconstructed, and, more importantly, the artifacts in recovered images are significantly reduced. DVSAO_TV behaves better than DVSAO_FA concerning the ISNR values. This outcome occurs mainly because the TV norm has a more powerful capacity to preserve the edge and textures of recovered images compared with the FA norm, which is also experimentally verified by the results obtained by VSPCG_TV and VSPCG_FA. The CPU time summarized in Table 1 represents the mean running time of the corresponding approach when an observed image in Figure 2 is repeatedly recovered 10 times. Based on time consumption, the approaches with the TV regularizer are faster than those with the FA

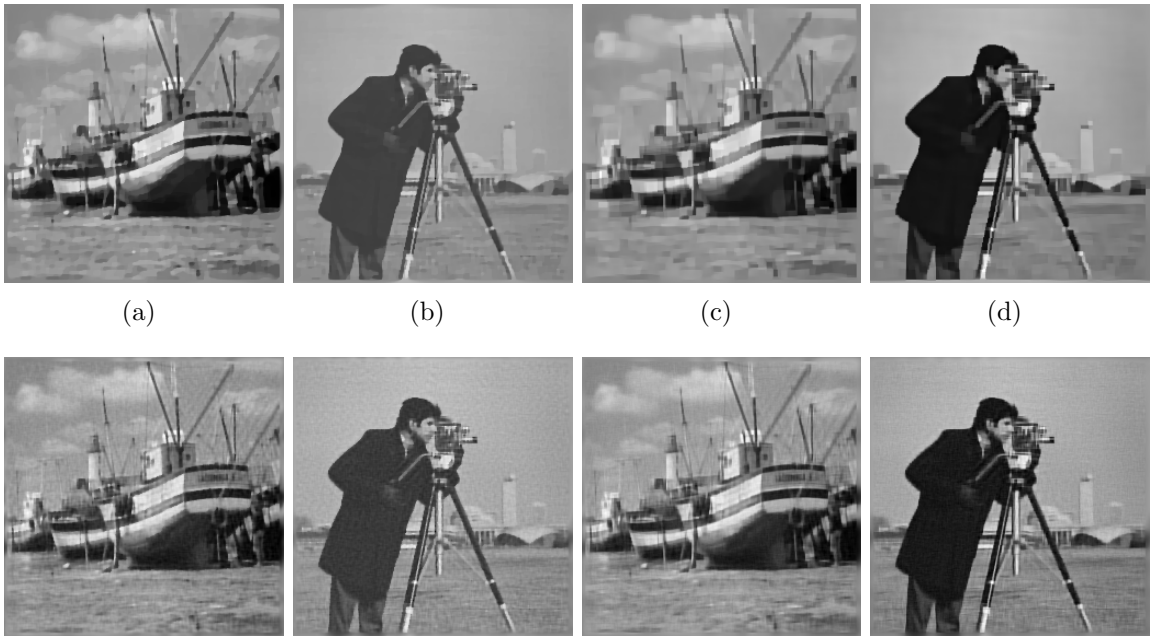

(a) (b) (c) (d)

(e) (f) (g) (h)

FIGURE 3. Images recovered by all approaches: (a)-(b) images recovered by VSPCG_TV, (c)-(d) images recovered by VSPCG_FA, (e)-(f) images recovered by DVSAO_TV, and (g)-(h) images recovered by DVSAO_FA

TABLE 1. ISNR values of recoveries and average time consumed

Approaches	**Boat**	**Cameraman**	**CPU Time**
VSPCG_TV	5.57 dB	6.37 dB	18.72 s
VSPCG_FA	4.28 dB	5.06 dB	29.83 s
DVSAO_TV	6.90 dB	7.03 dB	10.24 s
DVSAO_FA	6.59 dB	6.83 dB	12.20 s

regularizers because the redundant Haar frame with four-level decomposition used in this study slows down the latter. PCG requires more iterations to converge, which negatively affects the speed of image recovery, and it cannot provide exact solutions. Compared with the VSPCG approach, the DVSAO approach demonstrates better overall performance in terms of visual effects, ISNR values, and time consumption. To analyze the convergences of all approaches, the comparisons of changes of cost functions $0.5\times||y-HBx||_2^2+\mu\Phi(Px)$ are plotted in Figure 4. The figure illustrates that, to converge to a solution that satisfies $\left(||x^{k+1}-x^k||_{fro}/||x^k||_{fro}\right) < 1\times 10^{-4}$, the presented DVSAO approach needs fewer than 100 iterations, whereas the VSPCG approach needs significantly more iterations to do so.

5. **Conclusions.** This paper presents a novel DVSAO approach to solve the image recovery problem (3) under an unknown condition. Based on double variable splittings and alternating optimization, several subproblems are alternately and iteratively computed to obtain the solutions to the problem (3). To validate the presented approach, experiments on recovering uniform-blurred images are performed. The recovered images, ISNR values, and time consumption demonstrate the validity of the presented approach and its advantages over similar VSPCG approaches. Future work involves extending the presented approach to deal with image inpainting problems, which share numerous similarities with image recovery problems under unknown boundary conditions.

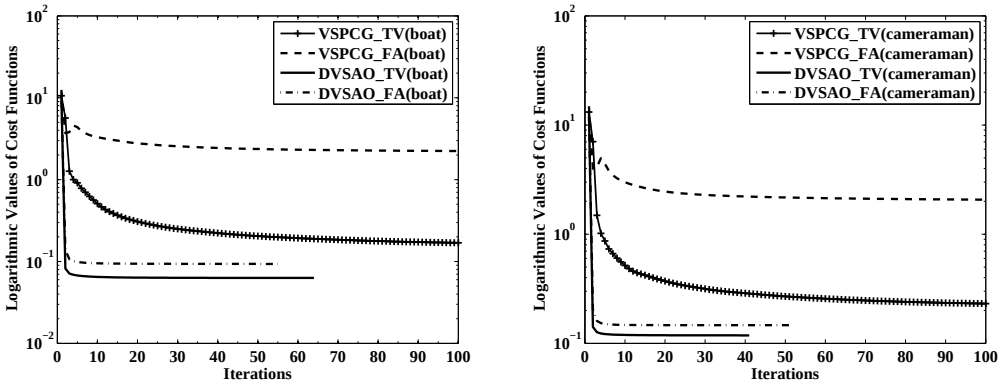

FIGURE 4. Changes of cost functions

Acknowledgment. This work is supported by Anhui Provincial Natural Science Foundation (No. 1608085QF150).

REFERENCES

[1] J. Yang, W. Yin, Y. Zhang and Y. Wang, A fast algorithm for edge-reserving variational multichannel image restoration, *SIAM Journal on Imaging Sciences*, vol.2, no.2, pp.569-592, 2009.

[2] A. Beck and M. Teboulle, Fast gradient-based algorithms for constrained total variation image denoising and deblurring problems, *IEEE Trans. Image Processing*, vol.18, no.11, pp.2419-2434, 2009.

[3] O. V. Michailovich, An iterative shrinkage approach to total-variation image restoration, *IEEE Trans. Image Processing*, vol.20, no.5, pp.1281-1299, 2011.

[4] Y. Chen, W. W. Hager, M. Yashtini, X. Ye and H. Zhao, Bregman operator splitting with variable stepsize for total variation image reconstruction, *Computational Optimization and Applications*, vol.54, no.2, pp.317-342, 2013.

[5] Y. Yang, M. Moller and S. Osher, A dual split Bregman method for fast l^1 minimization, *Mathematics of Computation*, vol.82, no.284, pp.2061-2085, 2013.

[6] R. H. Chan, M. Tao and X. Yuan, Constrained total variation deblurring models and fast algorithms based on alternating direction method of multipliers, *SIAM Journal on Imaging Sciences*, vol.6, no.1, pp.680-697, 2013.

[7] T. Goldstein, B. O'Donoghue, S. Setzer and R. Baraniuk, Fast alternating direction optimization methods, *SIAM Journal on Imaging Sciences*, vol.7, no.3, pp.1588-1623, 2014.

[8] T. F. Chan, A. M. Yip and F. E. Park, Simultaneous total variation image inpainting and blind deconvolution, *SIAM Journal on Imaging Sciences*, vol.15, no.1, pp.92-102, 2005.

[9] S. J. Reeves, Fast image restoration without boundary artifacts, *IEEE Trans. Image Processing*, vol.14, no.10, pp.1448-1453, 2005.

[10] M. Sorel, Removing boundary artifacts for real-time iterated shrinkage deconvolution, *IEEE Trans. Image Processing*, vol.21, no.4, pp.2329-2334, 2012.

[11] T. F. Chan and S. Esedoglu, Aspects of total variation regularized L1 function approximation, *SIAM Journal on Applied Mathematics*, vol.65, no.5, pp.1817-1837, 2005.

[12] J. F. Cai, B. Dong, S. Osher and Z. Shen, Image restoration: Total variation, wavelet frames, and beyond, *Journal of the American Mathematical Society*, vol.25, no.4, pp.1033-1089, 2012.

[13] M. Zhu, S. J. Wright and T. F. Chan, Duality-based algorithms for total-variation-regularized image restoration, *Computational Optimization and Applications*, vol.47, no.3, pp.377-400, 2010.

[14] N. Pustelnik, J. C. Pesquet and C. Chaux, Relaxing tight frame condition in parallel proximal methods for signal restoration, *IEEE Trans. Signal Processing*, vol.60, no.2, pp.968-973, 2012.

[15] X. Ye, Y. Chen and F. Huang, Computational acceleration for MR image reconstruction in partially parallel imaging, *IEEE Trans. Medical Imaging*, vol.30, no.5, pp.1055-1063, 2011.

[16] N. Parikh and S. Boyd, Proximal algorithms, *Foundations and Trends in Optimization*, vol.1, no.3, pp.127-239, 2014.

[17] K. Bredies and D. A. Lorenz, Linear convergence of iterative soft-thresholding, *Journal of Fourier Analysis and Applications*, vol.14, nos.5-6, pp.813-837, 2008.